JOURNAL OF MATERIALS SCIENCE **36** (2001) 1863–1871

Some observations on the effect of austenitisation conditions on the transformation kinetics in an HSLA steel and related C-Mn steels

T. A. KOP, P. G. W. REMIJN*, V. SVETCHNIKOV, J. SIETSMA, S. VAN DER ZWAAG
Laboratory for Materials Science, Rotterdamseweg 137, 2628 AL Delft, The Netherlands
E-mail: sietsma@tnw.tudelft.nl

The dependence of the transformation kinetics of an HSLA steel and related C-Mn steels on the austenitisation conditions have been investigated using calorimetry and dilatometry. It is observed that the ferrite-start temperature depends both on the manganese content and on the amount of niobium in solution. Calculations of the transformation kinetics based on an interface-mobility model applied in a tetrakaidecahedron austenite-grain geometry are used to investigate the background of the observed changes in transformation kinetics.

1. Introduction

Transformation kinetics in modern construction steels are rather complex. The austenite to ferrite phase transformation depends on the chemical composition of the steel, on the austenite microstructure before transformation and on the applied cooling rate. The microstructure that results after transformation depends on the combined effect of the above-mentioned factors.

The effects of chemical composition are threefold. Carbon, the main interstitial alloying element, will pile up at the migrating austenite/ferrite interface due to the limited carbon solubility in ferrite, thereby reducing the local driving force for transformation. Substitutional elements like manganese and silicon also have a strong effect on the transformation kinetics. High concentrations of substitutional elements give rise to deeper undercooling, thereby giving rise to the formation of Widmanstätten ferrite and bainite rather than allotriomorphic ferrite. Some alloying elements form precipitates at austenitisation temperatures. These precipitates can inhibit grain growth, thereby causing a reduced austenite grain size.

The starting microstructure for the transformation, which is characterised by the austenite grain size and the amount of alloying elements either in solute solution or in precipitated form, depends on the preceeding time-temperature path. It is well known that there is a relation between the reheat temperature and the austenite grain size. In the case of HSLA steels the time-temperature path also determines the amount and size of the precipitates [1, 2]. High temperature plastic deformation has a large influence on both the austenite grain size and the amount and spatial distribution of precipitates [3, 4].

The microstructure obtained when cooling down the austenite depends on the cooling rate. At low cooling rates there will be enough time for the formation of allotriomorphic ferrite. In this regime the chemistry of the system has a distinct influence on the nucleation and growth behaviour. At higher cooling rates there will be less time for the formation of allotriomorphic ferrite, and a transition to Widmanstätten ferrite formation will occur [5]. After ferrite formation there will be pearlite or bainite/martensite formation.

From the above it is clear that in an HSLA steel the chemistry and the austenite grain size are highly coupled. There are not many papers in the literature which actually study the growth kinetics of ferrite quantitatively and try to separate the influence of solute or precipitated niobium on nucleation or growth kinetics [6–8]. In the paper by Cochrane and Morrison [6] it is argued that precipitation before transformation accelerates the allotriomorphic ferrite formation. Thomas and Michal [7] have found a decrease in the ferrite-start temperature for niobium contents less than 0.04 wt.%, and an increasing ferrite-start temperature for higher niobium concentrations. Lee *et al.* [8] model and discuss the growth kinetics on the basis of the classical nucleation and diffusional growth theories. It is concluded that the solute niobium slows down the ferrite-start and that solute and precipitated niobium have the same effect on the progress of the ferrite formation.

In the work presented here a comparison between the transformation kinetics of a niobium containing steel and similar C-Mn steel grades without niobium is made. Furthermore, several series of experiments on the niobium containing steel are performed to separate the effects of precipitated niobium and niobium in solution. Experiments to determine the transformation kinetics are performed using both Differential Thermal Analysis (DTA) and dilatometry, while microstructural data are obtained using optical microscopy and Transmission Electron Microscopy (TEM).

* *Present Address*: Corus UK Limited, Swinden Technology Centre, Rotherham, S60 3AR, United Kingdom.

An analysis of the transformation kinetics is performed in terms of an interface mobility model which incorporates microstructural features such as austenite grain size and nucleation site density [9].

2. Theory

A key property for the effect of niobium on the formation of both the austenite and the ferrite microstructure is the solubility product of niobium-(nitro)carbide [10]. In the present study we will concentrate on NbC as the precipitating phase. The solubility product k for NbC is defined by

$$k = [\mathrm{Nb}][\mathrm{C}], \tag{1}$$

in which [A] denotes the concentration of element A in solution in the iron lattice. Most commonly, [A] is expressed in weight percentages. The solubility product has an Arrhenius-like temperature dependence, which is expressed by the equation

$$k = k_0 \exp\left(-\frac{Q_s}{RT}\right), \tag{2}$$

with k_0 denoting a pre-exponential factor, Q_s an activation energy, R the gas constant and T the temperature. From Equation 1 and the total amount of niobium in the alloy the weight percentage of Nb present as NbC-precipitate, c_{NbC}, can be readily derived.

Several sets of the parameters k_0 and Q_s for NbC in ferrite and in austenite have been proposed in the literature, as summarised recently by Gladman [11]. Whereas the actual values for k_0 and for Q_s show considerable differences, the resulting values for k as a function of T show that the variation in k in the austenite temperature range ($1000\ \mathrm{K} < T < 1300\ \mathrm{K}$) is limited to $\pm 30\%$. For ferrite ($800\ \mathrm{K} < T < 1200\ \mathrm{K}$) the differences increase up to $\pm 60\%$. In this work we will adopt the values $k_0 = 1380$ (wt.%)^2 and $Q_s = 148$ kJ/mol for the austenite phase, which were derived from the SGTE thermodynamic database. The parameters for the solubility product of NbC in ferrite have the values $k_0 = 31600$ (wt.%)^2 and $Q_s = 194$ kJ/mol. For the HSLA steel grade (0.02% Nb) used in this work it follows that for $T > 1350$ K all niobium dissolves in the austenite phase (Fig. 1). In the ferrite phase the solubility is less than in the austenite phase. At temperatures at which ferrite is stable the formation of niobium carbide precipitates is thermodynamically favourable.

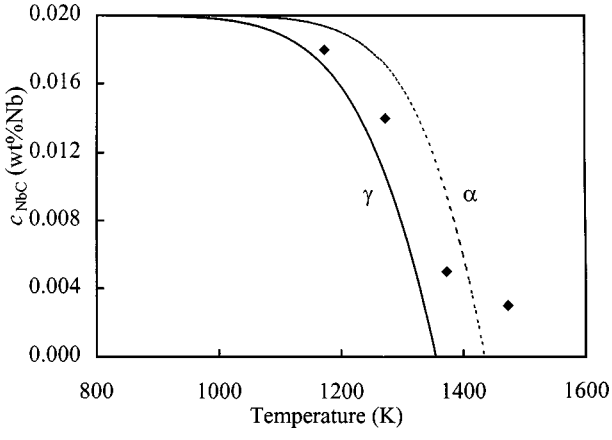

Figure 1 Equilibrium concentration of niobium-carbide precipitates in austenite (γ) and ferrite (α) as a function of temperature for 0.02% Nb steel. The symbols denote the experimentally determined values.

There are several models available to describe the austenite to ferrite phase transformation. In the work presented here the aim is to obtain a better understanding of the physical processes occurring during -and thereby governing- the austenite to ferrite phase transformation. Therefore a physically based model is used. A first quantity to consider in the model is the size and the shape of the austenite grains. The austenite grains have irregular three-dimensional shapes, corresponding with a Voronoi tesselation, which on average contain approximately 15 faces. Van Leeuwen *et al*. [9] describe a model which is based on a tetrakeidecahedron, which can be regarded as an average austenite grain shape. In this geometry, nucleation can be simulated to take place at specific sites, for instance the austenite grain corners, from which the nuclei grow spherically into the austenite grain. The fraction ferrite as a function of time is determined by numerical integration.

In order to simulate the growth of the ferrite grains, the interface mobility model as described by Krielaart *et al*. [12], after Christian [13], is used. The interface velocity v is given by the product of the interface mobility M and the driving force for transformation, $\Delta G^{\gamma/\alpha}$, according to

$$v = M \cdot \Delta G^{\gamma/\alpha} = M_0 \exp\left(-\frac{Q}{RT}\right) \cdot \Delta G^{\gamma/\alpha}, \tag{3}$$

where M_0 is a pre-exponential factor, Q the activation energy for movement of the atoms in the boundary region, and $\Delta G^{\gamma/\alpha}$ is the difference in Gibbs free energy between the austenite and the ferrite. In this work we will adopt this definition of interface velocity. The driving force can be calculated using a thermodynamic database, which takes into effect the contributions of manganese and carbon. The manganese is assumed to be homogeneously distributed throughout the material. Furthermore it is assumed that the carbon redistributes during the austenite to ferrite transformation, and that the carbon is distributed homogeneously throughout the austenite phase. The total amount of niobium present in the system is too small to have a noticeable influence on the phase diagram and the resulting driving force. The principal influence of the chemical composition is thus incorporated.

If precipitates are present, they can influence the transformation kinetics, for instance by exerting a pinning force on the austenite/ferrite interface, effectively reducing M_0. According to the classical Zener approach [14] the Zener drag or Zener retardation pressure P_z, experienced by a moving interface and caused by a distribution of precipitates, is given by

$$P_z = \frac{3}{4}\beta\frac{f\gamma}{r}, \tag{4}$$

where β is a correction factor, γ is the interfacial energy, f the volume fraction of precipitates and r the size of the precipitates. Spherical incoherent precipitates were

assumed and the problem is treated only geometrically. In this case β equals 1. In later studies the correction factor β was introduced [15]. This factor can vary between 0.1 and 2.3, depending on the geometry of the precipitates and the shape of the deforming grain boundary.

The parameters describing the interface mobility, M_0 and Q, are mathematically strongly correlated when Equation 2 is fitted to experimental data on the kinetics of the phase transformation. The approach adopted in this study is to keep the activation energy at a fixed value and to vary the pre-exponential factor to optimise the agreement between experimental and modelled fraction curves. For the activation energy a value of 140 kJ/mol is used. This value corresponds with the activation energy for austenite recrystallisation [16] and to the value used by Krielaart and van der Zwaag for the austenite to ferrite transformation in binary Fe-Mn alloys [12]. Factors that do influence the transformation kinetics but have not been incorporated in the model will affect the value of the pre-exponential factor, M_0.

In the calculations it is assumed that nucleation takes place instantaneously at a certain temperature during cooling from the austenitisation temperature. The undercooling, ΔT, is defined as the difference between this temperature and the Ae_3-temperature. The undercooling, which is a measure for the delay in nucleation, is also varied to optimise the correspondence between calculated and measured data.

3. Experimental

The compositions of the steel grades used in this investigation are given in Table I. Grade Mn12Nb is the HSLA steel, and contains a small amount of niobium, 0.02 wt.%, and furthermore as main alloying elements 1.20 wt.% manganese and 0.136 wt.% carbon. The other grades do not contain niobium, but differ in manganese, carbon and silicon concentration. The grades are coded according to the manganese content. The compositions lead to a variation in the equilibrium fractions as a function of temperature, as can been seen in Fig. 2. In this figure the total fraction of ferrite plus pearlite for the different steel grades is shown as a function of temperature in the ferrite/austenite region. The fractions are calculated using the thermodynamic database program MTData assuming para-equilibrium and taking into account contributions of manganese, silicon and carbon. The relatively low Ae_3-temperature of the Mn11 alloy is caused by the relatively high carbon concentration.

For the quantitative analysis of the fractions solute and precipitated niobium as a function of the austenitisation temperature, samples were electrochemically brought into solution using an EDTA solution. In this process the precipitates do not dissolve. The electrolyte is filtered using a filter with a 100 nm pore size. The residue is mixed with Na_2SO_4. This mixture is melted and dissolved in a solution of sulphuric and oxalic acid. The niobium concentration of this solution as well as the niobium concentration in the electrolyte are determined using a Perkin Elmer Inductive Coupled Plasma – Optical Emission Spectrometer (ICP-OES).

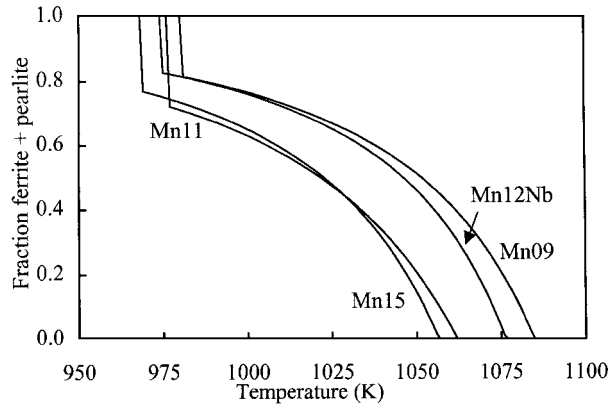

Figure 2 Equilibrium ferrite plus pearlite fraction as a function of temperature for the steel grades presented in Table I.

To obtain data on the transformation kinetics, dilatometry experiments were performed using a Bähr 805A/D dilatometer. Cylindrical samples of 4.0 mm diameter and 10.0 mm length were clamped between quartz push-rods. The samples were heated by induction and the temperature was registered by S-type thermocouples. The temperature gradients along the length of the samples remained within 10 K. Cooling rates were controlled to be constant over the entire transformation range. For the higher cooling rates an N_2-flow was used. The dilatation data were analysed using a method that accounts for the difference in specific volume between ferrite and cementite [17]. Three series of experiments were performed. The first series was performed at different austenitisation temperatures, ranging from 1173 K to 1423 K, in order to determine the dependence of the austenite grain size and the subsequent transformation kinetics on the austenitisation temperature. The samples were heated at a rate of 50 K/min, held for 20 minutes at the austenitisation temperature, and cooled at 20 K/min. To investigate the influence of different austenitisation times, a second series of experiments was performed, consisting of heating at 5 K/s to 1423 K, an isothermal hold for 5, 20 or 40 minutes and subsequent cooling at 20 K/min. Finally, two

TABLE I Chemical composition of alloys (wt%)

Alloy	%C (at.%)	%Mn	%Si	%Nb	%Al	%Cr	%Mo	%Ni	%Cu	%N	%S	%P
Mn12Nb	0.136 (0.63)	1.200	0.017	0.020	0.053	0.025	0.002	0.027	0.013	0.0036	0.009	0.016
Mn09	0.147 (0.68)	0.926	0.009	0.002	0.043	0.027	0.004	0.026	0.016		0.010	0.011
Mn11	0.210 (0.98)	1.100	0.320	<0.005	0.028	<0.02	<0.005	0.020	<0.02	0.0077	0.008	0.011
Mn15	0.173 (0.80)	1.460	0.178	-	0.031	-	0.002	0.026	0.011	0.0064	0.008	-

different types of two-step annealing experiments were made. The samples were first annealed at 1423 K to dissolve the niobium-carbide precipitates, and the second anneal was performed at a temperature below the precipitation start temperature (1350 K) to allow for re-precipitation of the niobium carbide. Analogous experiments were performed without the second anneal, yielding samples with the same austenite grain size, but a different amount of niobium in solution. The first type of the two-step annealing experiments -heat treatment A- consisted of heating at a rate of 50 K/min, annealing for 20 minutes, cooling at 20 K/min to 1273 K, holding for 0 or 30 minutes and subsequent cooling at 20 K/min. The other heat treatment -heat treatment B- consisted of heating at 5 K/s, annealing for 40 minutes, cooling at 10 K/s to 1033 K, holding for 0, 30 or 60 minutes and subsequent cooling at 20 K/min. The experiments with varying austenitisation temperature as well as one of the two-step annealing experiments were also performed on a Perkin-Elmer DTA-7 apparatus. Discs with a diameter of 3.0 mm and a height of 2 mm were used. Special care was taken to prevent decarburisation by using a purified N_2-gas flow through the sample chamber. Microstructural data were obtained using optical microscopy. 2% nital was used to reveal the ferritic/pearlitic microstructures. The prior austenite grain boundaries were revealed using both a thermal etching technique and a technique based on the partial transformation of the sample. The grain sizes were determined using the mean linear intercept method.

The TEM foils were prepared by mechanical grinding, electropolishing and ion-milling. A Philips CM30 TEM was used to detect niobium-carbide precipitates. Both bright and dark field techniques were applied.

4. Results and discussion

4.1. Experimental

Fig. 1 shows c_{NbC} in the austenite and in the ferrite phase as a function of temperature, calculated from the solubility products for the HSLA-steel investigated in this study. The concentration of precipitated niobium after austenitisation at the indicated temperatures (followed by a quench to room temperature), as found by the chemical analysis, is depicted as well. The measured results correspond well with the calculated results, although the experimental concentrations are slightly higher than the theoretical values. The theoretical values describe the equilibrium case. The experimentally observed concentrations however, are influenced by the kinetics of the dissolution of the niobium carbides. It can be seen that above 1350 K most niobium is dissolved in the austenite phase. At this temperature a bimodal austenite grain size distribution is observed in optical microscopy. This bimodal austenite grain size distribution is due to the transition of grain growth inhibited by pinning by the precipitates of normal grain growth after the dissolution of the precipitates, as is described in [18]. For the steel grades without niobium no bimodal austenite grain size distribution is found. Combining Figs 1 and 2 it can been seen that according to equilibrium predictions all niobium should be precipitated before the austenite to ferrite transformation starts, since the Ae_3-temperature for Mn12Nb is 1078 K.

Figs 3 and 4 show the effect of the austenitisation temperature on the transformation kinetics as observed by DTA and dilatometry. Fig. 3 shows the DTA measurements and Fig. 4 shows the measured dilatation and the resulting fraction transformed during cooling for alloy Mn12Nb. The DTA measures the specific heat and the transformation enthalpies. Therefore the sensitivity for the ferrite formation becomes larger at lower

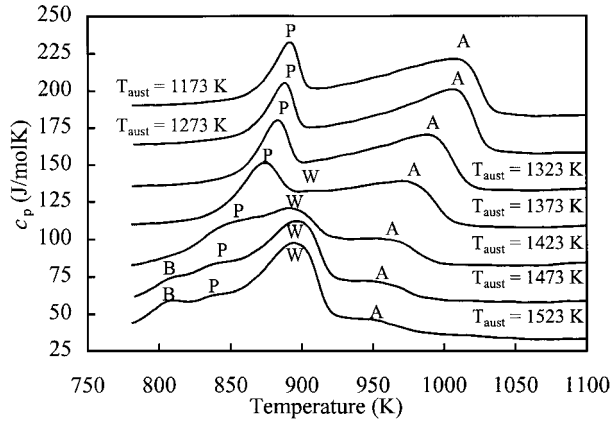

Figure 3 The measured specific heat curves (plus a multiple of 25 J/molK for all except the lowest curve) during cooling at 0.3 K/s after austenitising Mn12Nb at different temperatures, as measured with the DTA. The labels A, W, P, and B correspond to the formation of allotriomorphic ferrite, Widmanstätten ferrite, pearlite and bainite respectively.

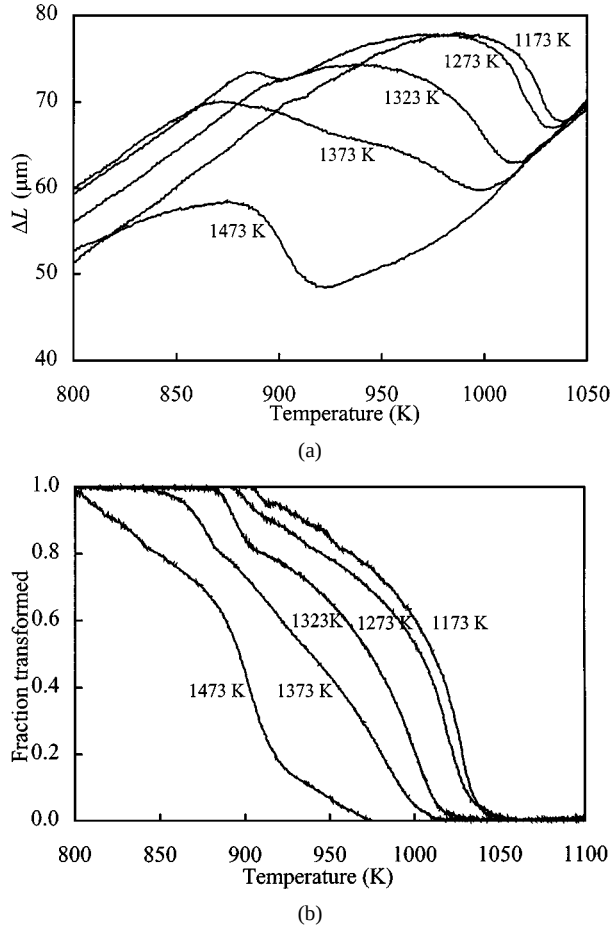

Figure 4 (a) The dilatation curves, and (b) the fractions transformed of Mn12Nb during cooling at 0.3 K/s after austenitisation at different temperatures. The austenitisation temperature is indicated.

temperatures. The sensitivity for the pearlitic reaction is even larger, caused by the formation of the covalent cementite structure. The height of a peak is a measure for the average rate of the transformation, $\mathrm{d}f/\mathrm{d}T$ [19]. In Fig. 3 a multiple of 25 J/molK is added to each measured heat curve in order to clarify the relative changes between the curves belonging to different austenitisation temperatures.

In the DTA signal corresponding to the lowest austenitisation temperature, 1173 K, two peaks, labelled A and P, are observed. It is seen that the allotriomorphic ferrite formation (peak A) starts at 1050 K. The second peak, corresponding to the pearlite formation starts at 905 K (peak P). The heat effect measured after the highest austenitisation temperature indicates four different processes. The peak corresponding to the allotriomorphic ferrite formation is still present, shifted towards lower temperatures and smaller with respect to the A-peak after the lowest austenitisation temperature. The largest peak in this curve, peak W, starting at 925 K, corresponds to the formation of Widmanstätten ferrite. This peak partly overlaps with the peak corresponding to the pearlite formation. The peak at 810 K, labelled B, corresponds to bainite formation. The peak labelling was applied on the basis of microstructural analysis of the fully transformed samples. Fig. 3 shows that increasing the austenitisation temperature shifts the ferrite start temperature towards lower temperatures. Furthermore, it is seen that at higher austenitisation temperatures the formation of Widmanstätten ferrite becomes favourable because less allotriomorphic ferrite is formed. The appearance of the Widmanstätten phase coincides with the niobium-carbide precipitates being dissolved (i.e. above 1350 K).

The dilatation signal (Fig. 4a) can be used to obtain data concerning the phase fractions, since the phase transformation results in volume changes. The volume change corresponding to the austenite to ferrite transformation depends on the carbon concentration of the austenite, and since the volume change corresponding to the austenite to pearlite transformation is normally less than the volume change of the austenite to ferrite transformation, the pearlite formation is less clearly observable. Nevertheless the dilatation signal shows the same features as the DTA results. Fig. 4a gives the measured change in length. The dilatation curves are shifted along the ΔL-axis such that they coincide in the austenite region and highlight the shift in transformation start temperature. The absolute length change is difficult to measure accurately and depends on the sample preparation [20]. Fig. 4b shows the fraction transformed curves obtained from the dilatation measurements. For the specimen austenitised at 1173 K both allotriomorphic ferrite and pearlite formation are detectable in the dilatation signal. The specimen austenitised at 1473 K shows some allotriomorphic ferrite formation before a transition to Widmanstätten ferrite occurs. Note that the formation of Widmanstätten ferrite, which was visible as a peak in the DTA-signal, shows as an increase of the length-change rate in dilatometry. In this sample both pearlite and bainite are formed. In the dilatation signal however it is not possible to distinguish the pearlite from the bainite formation.

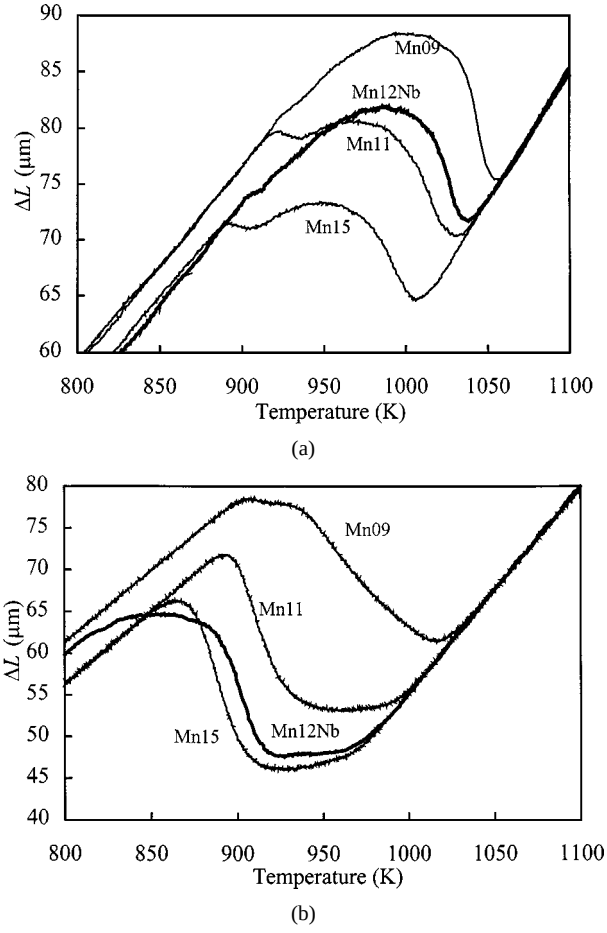

Figure 5 Dilatation curves for the four steel grades investigated after austenitisation (a) at 1173 K, and (b) at 1423 K.

Fig. 5a shows the dilatation curves of the steel grades investigated, all austenitised at 1173 K and subsequently cooled at a rate of 0.3 K/s. They indicate that the average transformation rate of the steel grades is approximately the same. The transformation products are allotriomorphic ferrite and pearlite. Comparing the dilatation curves with the equilibrium fraction curves of Fig. 2, it is seen that the Mn15 alloy has the largest undercooling. This indicates that the retarding influence of manganese is larger than the influence of the carbon. Fig. 5b shows the dilatation curves after austenitisation at 1423 K. The transformation behaviour of Mn09 is quite similar as before. There is a rapid formation of allotriomorphic ferrite followed by the formation of pearlite. The other three alloys, however, show a slower formation of ferrite and a transition to the formation of Widmanstätten ferrite. The shift in ferrite-start temperature of Mn12Nb is quite large in comparison to the shift in ferrite-start temperature of Mn11 when the transformation kinetics after austenitisation at 1173 K and 1423 K are compared. Furthermore, there is a prominent retardation in the pearlite formation of the Mn12Nb alloy. Fig. 6 summarises the above. The shift of the experimentally determined start temperature relative to the equilibrium A_3 temperature for the steel grades investigated is plotted against the austenitisation temperature. The dashed lines as well as the low temperature part of the Mn12Nb line are all parralel and are intended as a guide to the eye. For the non-niobium containing alloys there is a gradual dependence between the undercooling and the austenitisation temperature,

TABLE II M_0, ΔT and d_γ as a function of the austenitisation time at 1423 K for the Mn12Nb steel grade. The corresponding experimental dilatation curves are shown in Fig. 7a

t_{aus} (min.)	M_0 (molmm/Js)	ΔT (K)	d_γ (μm)
5	18	60	193
20	22	70	245
40	30	100	309

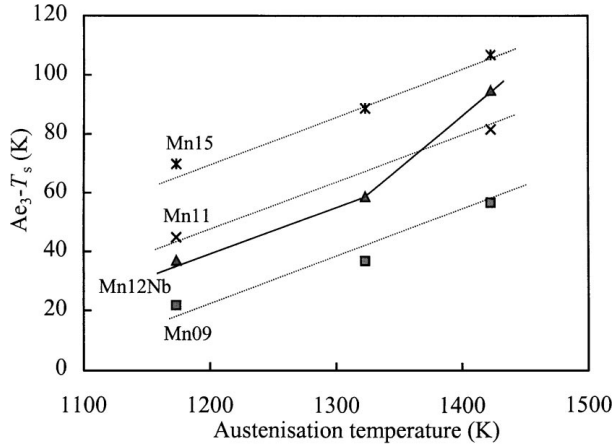

Figure 6 The shift of the experimentally determined start temperature (T_s) relative to the equilibrium A_3 temperature *vs.* the austenitisation temperature for the steel grades investigated.

whereas in the Mn12Nb alloy an additional retardation is observed for austenitisation above 1323 K.

The relation between the austenite grain size and the ferrite-start temperature is also observed when analysing the effect of the austenitisation time, as is seen in Fig. 7a for the Mn12Nb alloy and in Fig. 7b for Mn11. Both figures show a delay in the ferrite-start temperature. In Table II the austenite grain sizes of Mn12Nb are given, and it is seen that longer austenitisation times indeed lead to an increase in austenite grain size. A further comparison of Fig. 7a and b shows that even after a short austenitisation time, the ferrite growth rate in the Mn12Nb steel is effectively reduced. Furthermore due to the slow pearlite formation in the Mn12Nb steel, the transition of Widmanstätten ferrite to pearlite formation is clearly visible for this grade. An increase in cooling rate also leads to an increased undercooling, as can be seen in Fig. 8. This however is not caused by the austenite grain size, but by the time available for nucleation. Another interesting feature in Fig. 8 is the transition from allotriomorphic ferrite formation to Widmanstätten ferrite formation, which depends both on the transformation temperature and the amount of allotriomorphic ferrite formed.

Figs 9 and 10 show the DTA and dilatation measurements of the two-step annealing experiments. The holding temperature was chosen at 1273 K, such that precipitation of the niobium in NbC, which had gone into solute solution during austenitisation at 1423 K, is thermodynamically favourable. In order to determine the influence of the niobium, in Fig. 10 the fraction curves for Mn11 for identical heat treatments are also shown. For the Mn11 alloy there is no influence of the additional holding at 1273 K. This indicates that the austen-

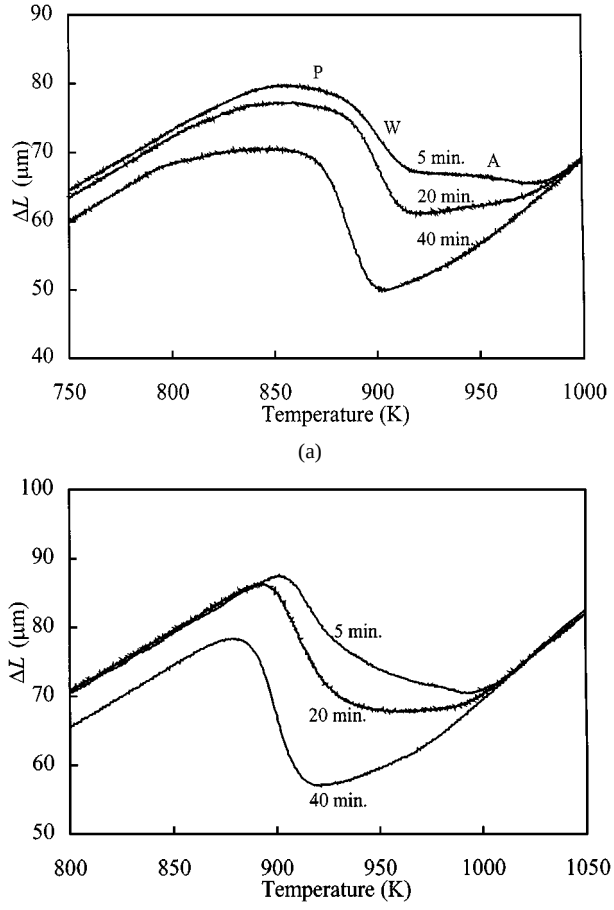

Figure 7 Dilatation curves resulting from different austenitisation times at 1423 K when a cooling rate of 0.3 K/s is applied for (a) steel grade Mn12Nb, and (b) steel grade Mn11.

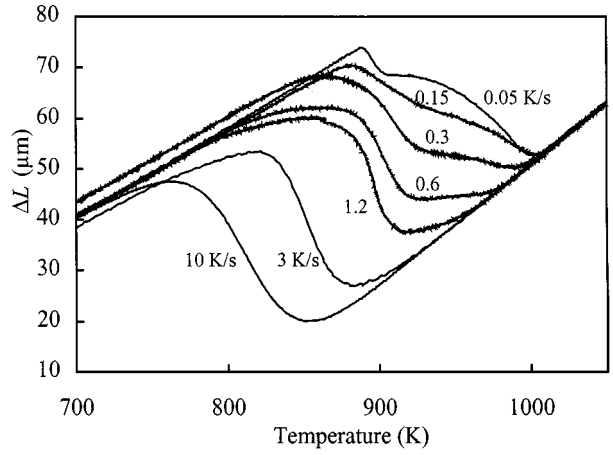

Figure 8 Dilatation curves for Mn12Nb for various cooling rates after austenitisation at 1423 K.

ite grain size does not change during the 1 hour hold. In the fraction curves corresponding to the niobium containing alloy there is a shift along the temperature axis; after the additional hold the ferrite-start temperature is increased. The amount of allotriomorphic ferrite formed is larger and the amount of Widmanstätten ferrite smaller. The specific heat curves show the same features. The shift in start temperature is less clearly visible, but the shift towards less Widmanstätten ferrite formation and thereby a reduced contribution to the heat effect of the Widmanstätten ferrite compared with

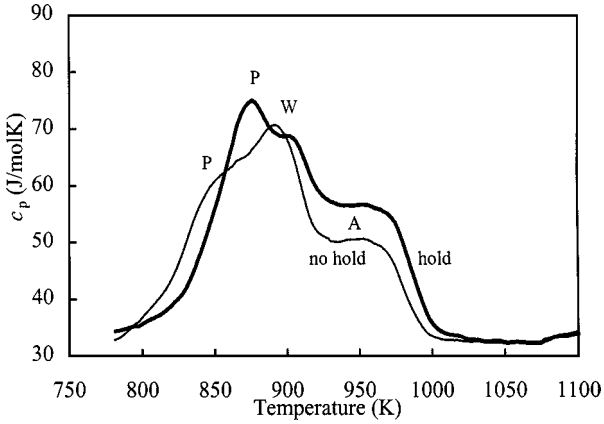

Figure 9 Specific heat curves for Mn12Nb. The peaks correspond to allotriomorphic ferrite, Widmanstätten ferrite and pearlite formation. Both curves correspond to samples austenitised at 1423 K. One sample was additionally held at 1273 K for 30 minutes before further cooling.

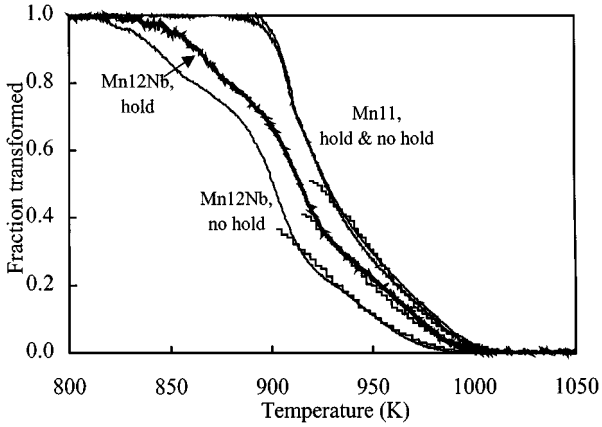

Figure 10 Fraction transformed for Mn12Nb and Mn11 after austenitising at 1423 K, with and without hold at 1273 K. The modelled allotriomorphic ferrite fractions are also given.

the contribution of pearlite is clear. Fig. 10 shows that the ferrite-start temperature after the additional hold is approximately 10 K higher than in the experiment without the intermediate hold. This corresponds to an undercooling of 85 K. Considering Fig. 6, it can be concluded that the net effect of the niobium in solution causes a retarding effect on the ferrite nucleation. The shift in start temperature is expected to be related to a change in the amounts of solute niobium and niobium

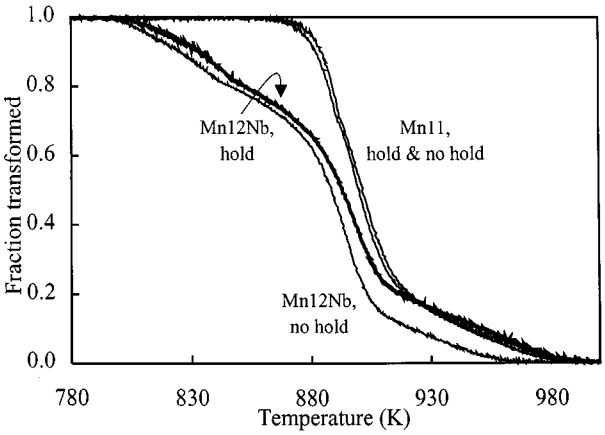

Figure 11 Fraction transformed for Mn12Nb and Mn11 after austenitising at 1423 K, with and without hold at 1033 K.

carbides. Fig. 11 shows the fractions transformed after holding at 1033 K, near the Ar_3 temperature, for alloys Mn12Nb and Mn11. The difference in average growth rate of the allotriomorphic ferrite between the curves in Figs 10 and 11 are due to the difference in austenite grain size, which is due to the variation in austenitisation time as was seen in Fig. 7. Apart from this difference the same observations are made as in Fig. 10: the additional hold for the Mn12Nb causes a reduction in undercooling while the hold has no influence on the transformation kinetics of the Mn11 alloy.

The TEM was used to compare the precipitation characteristics of the austenitisation treatments at 1423 K with and without the additional hold at 1033 K. Neither heat treatment led to precipitation on prior austenite grain boundaries nor to precipitation at the γ/α interface during transformation. The heat treatment without the additional hold resulted in a distribution of fine niobium-carbide precipitates. The heat treatment with the additional hold resulted, besides the fine precipitates, in numerous coarser particles. The coarseness of the precipitates indicates that they have been formed before the transformation occurred. Evidence of increased nucleation due to the presence of the precipitates is not observed. The delay in transformation-start temperature after the austenitisation above the precipitation-start temperature is probably due to the niobium in solution.

4.2. Model calculations

The model calculations focus on the behaviour of Mn12Nb. The results of the modelling are summarised in Tables II to IV. Fig. 10 shows an example of the model results. Both the undercooling, ΔT, and the pre-exponential factor, M_0, are varied, such that the modelled curves fit the part of the experimental fraction curves which corresponds to the allotriomorphic ferrite

TABLE III M_0 and ΔT as a function of the cooling rate after austenitisation at 1423 K for the Mn12Nb alloy. The corresponding experimental dilatation curves are shown in Fig. 8

β (K/s)	M_0 (molmm/Js)	ΔT (K)
0.15	9	35
0.3	16	45
0.6	28	55
1.2	50	70

TABLE IV M_0 and ΔT resulting from the two-step annealing experiments A and B. The corresponding experimental fraction curves are shown in Figs 10 and 11

Alloy	Holding temperature (K) & time (min.)	M_0 (molmm/Js)	ΔT (K)
Mn12Nb	1033/60	20	50
	1033/30	21	60
	1033/0	23	80
	1273/30	18	40
	1273/0	19	60
Mn11	1273/0	33	16
	1273/30	33	16

formation. The modelled curves are not smooth since a limited grid of $40 \times 40 \times 40$ is used in the numerical model.

Table III shows both an increasing M_0 and ΔT with increasing austenitisation temperature. The increase in ΔT is caused by the lower density of heterogeneous nucleation sites, due to the increase in d_γ. The increase in M_0, which corresponds with a higher interface velocity, might seem to contradict Fig. 7, where for the higher austenitisation temperature a lower $\mathrm{d}f/\mathrm{d}T$ was found. It should be noted however, that not only M_0, but also the nucleus density influences the overall $\mathrm{d}f/\mathrm{d}T$. The nucleus density however is hard to determine accurately. In all calculations, the number of 24 nuclei per austenite grain, corresponding to all the corners of the tetrakaidecahedron, was used. As an example of the influence of this choice, a calculation for the experiment consisting of the 40 minutes austenitisation treatment, with more nuclei, viz. 40 per austenite grain, leads to $M_0 = 23$ mol mm/Js when ΔT is kept at 100 K.

Table III shows both an increasing M_0 and ΔT with increasing cooling rate. In these experiments, the austenite grain size from which the allotriomorphic ferrite forms is the same for each cooling rate. The shift in undercooling can therefore not be attributed to the austenite grain size, and is most likely related to the time available for nucleation. The model calculations show a large cooling-rate dependence of the pre-exponential factor, implying a change in interface mobility. The main reason for this trend in M_0 is the increasing nucleus density, due to the lower ferrite-start temperature.

The data in Table IV are interesting since the holding experiments provide a means to separate the direct effect of the niobium on the transformation kinetics from austenite grain size effects. It is seen that the additional hold causes an increase in undercooling (see also Fig. 10). The growth rate however does not seem to be influenced significantly. The variation in M_0 is not significant. Fig. 12 shows the driving force for the transformation for the experiment with the one hour hold at 1033 K. It is seen that due to the low temperatures at which the transformation occurs, relatively large driving forces are involved, even for the low cooling rate used. One of the possible mechanisms by which the transformation could be slowed down is the pinning of the interface by precipitates. This pinning would result in a modification of the driving force as given by the difference in free energy between the ferrite and the austenite. The order of magnitude for the pinning force can be calculated using Equation 4. Assuming $\gamma = 0.2$ J/m^2 for an austenite/ferrite interface, $f = 2 \times 10^{-4}$, $r = 5 \times 10^{-9}$ m, $\beta = 1$ it follows that the pinning force is 0.04 J/mol. This value changes slightly for other values of β, γ, f or r, but it can always be neglected when compared to the driving forces involved. In Table IV the M_0 and ΔT values following from the fitting of the data of the Mn11 steel grade after austenitisation at 1423 K are also shown. The ΔT value is the lowest found in this work, which once more indicates the delay of nucleation in the niobium containing steel after austenitisation above the niobium-carbide dissolution temperature. Furthermore it is seen that the interface mobility of Mn11 is higher than that of Mn12Nb.

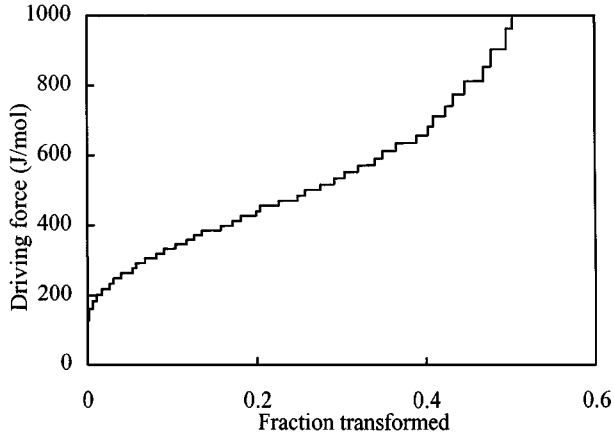

Figure 12 The driving force for transformation *vs*. allotriomorphic ferrite fraction as calculated for the two-step annealing experiment on Mn12Nb in which a 1 hour hold at 1033 K was applied.

5. Conclusions

A comparison of the transformation kinetics of an HSLA steel grade and related C-Mn alloys shows that, for the niobium containing steel, increasing the austenitisation temperature leads to a lower ferrite-start temperature and a transition to Widmanstätten ferrite formation. Also longer austenitisation times, leading to a reduction of heteregeneous nucleation sites, or higher cooling rates, delay nucleation and shift the transformation towards lower temperatures. The nucleus density however seems to increase. For the non-niobium containing alloys a retardation effect of manganese on the nucleation is observed. Also niobium in solution has a strong influence on the nucleation of ferrite as is shown by the shift of the ferrite-start temperature of the HSLA steel after an additional hold below the precipitation-start temperature, together with the relatively large shift of the undercooling as a function of the austenitisation temperature compared with the non-niobium containing alloys. The interface velocity of the austenite-ferrite interface itself is not changed by the change in the ratio between the amount of niobium in precipitates and the amount of niobium in solution.

Acknowledgments

The IOP-Metals program and the Netherlands Institute for Metals Research (NIMR) are gratefully acknowledged for financial support, the Corus group for the provision of material, and furthermore the people of the microscopic laboratory and chemical analysis group of the Laboratory for Materials Science, Delft.

References

1. W. J. LIU, E. B. HAWBOLT and I. V. SAMARASEKERA, in Conf. Proc. of Mathematical Modelling of Hot Rolling of Steel, Hamilton, Canada, 26–29 Augustus (1990), The Canadian Institute of Mining and Metallurgy, Montreal, p. 477.
2. P. A. MANOHAR, D. P. DUNNE, T. CHANDRA and C. R. KILLMORE, *ISIJ International* **36** (1996) 194.
3. B. DUTTA, E. VALDES and C. M. SELLARS, *Acta Metall. Mater*. **40** (1992) 653.
4. S. H. PARK, S. YUE and J. J. JONAS, *Metall. Trans. A* **23A** (1992) 1641.

5. R. L. BODNAR and S. S. HANSEN, *Metall. Mat. Trans. A* **25A** (1994) 665.
6. R. C. COCHRANE and W. B. MORRISON, in Conf. Proc. of Steels for Line Pipe and Pipeline Fittings London, 21st–23rd October (1981), The Metals Society, London p. 70.
7. M. H. THOMAS and G. M. MICHAL, in Proc. Int. Conf. on Solid to Solid Phase Transformations, edited H. I. Aaronson, D. I. Laughlin, R. F. Sekerka and L. M. Wayman, The Metallurgical Society of AIME, Warrendale, Pennsylvania, August 10–14 (1981) p. 469.
8. K. J. LEE, J. K. LEE, K. B. KANG and O. KWON, *ISIJ International* **32** (1992) 326.
9. Y. VAN LEEUWEN, S. I. VOOIJS, J. SIETSMA and S. VAN DER ZWAAG, *Met. Mat. Trans. A* **29A** (1998) 2925.
10. H. NORDBERG and B. ARONSSON, *I.S.I.J.* **206** (1968) 1263.
11. T. GLADMAN, "The Physical Metallurgy of Microalloyed Steels" (Institute of Metals, London, 1996).
12. G. P. KRIELAART and S. VAN DER ZWAAG, *Mat. Sci. Tech.* **14** (1998) 10.
13. J. W. CHRISTIAN, "The Theory of Transformations in Metals and Alloys, 2nd ed., (Pergamon Press, Oxford, 1981) p. 476.
14. C. ZENER as quoted by C. S. Smith, *Trans. AIME* **175** (1948) 15.
15. C. H. WÖRNER and P. M.HAZZLEDINE, *JOM* **44** (No. 9) (1992) 16.
16. M. HILLERT, *Metall. Trans.* **6A** (1975) 5.
17. T. A. KOP, J. SIETSMA and S. VAN DER ZWAAG, *J. Mat. Sci.* **36** (2001) 519.
18. E. J. PALMIERE, C. I. GARCIA and A. J. DEARDO, *Met. Mat. Trans. A* **25A** (1994) 277.
19. H. J. BORCHARDT and F. DANIELS, *J. Am. Chem. Soc.* **79** (1957) 41.
20. T. A. KOP, PhD thesis, Delft University of Technology 2000.

Received 26 April
and accepted 18 September 2000